



IONPs-induced neurotoxicity via cascade of neuro-oxidative stress, parthanatos-mediated cell death, neuro-inflammation and neurodegenerative changes: Ameliorating effect of rosemary methanolic extract

Arwa A. Elsheikh^a, Noha Ali Abd-Almotaleb^b, Mona Mostafa Ahmed^c,
Eman El-Sayed Khayal^{a,*} 

^a Forensic Medicine and Clinical Toxicology Department, Faculty of Medicine, Zagazig University, Egypt

^b Anatomy and Embryology Department, Faculty of Medicine, Zagazig University, Zagazig, Egypt

^c Pathology Department, Faculty of Medicine, Zagazig University, Zagazig, Egypt

ARTICLE INFO

Keywords:

IONPs
rosemary
PARP-1
AIF
 α -S
occludin

ABSTRACT

Iron oxide nanoparticles (IONPs) are widely used in various fields, particularly in medicine, where they can be directly injected for diagnostic and therapeutic purposes, although they may induce certain types of toxicity. Therefore, the present work aimed to estimate the potential protective role of the oral extract of rosemary (RO) against the toxic effects of injected IONPs on the brain tissues of adult male rats, and to explore the potential underlying mechanisms involved in reversing such toxicity. Thirty adult male albino rats were allocated into five groups: the control, the vehicle (intravenous saline injection once/week), the RO extract group (orally gavaged 100mg/kg/day), IONPs (intravenously injected 30 mg/kg once/week), and the combined RO+IONPs (orally gavaged RO extract 1 hrh before intravenous injection of IONPs). IONPs induced neurotoxicity via triggering a cascade of neuro-oxidative stress, neuro-inflammation, and parthanatos-mediated neuronal cell death by increasing MDA, NO, TNF- α levels, PARP-1, AIF, and NF- κ B mRNA expression alongside reducing GSH levels. These incidents contributed to neurodegenerative changes, reflected in increased mRNA expression of α -S, β -APP, and TDP-43. Additionally, IONPs induced structural degenerative changes and elevated iron levels in brain tissues reduced occludin expression, and disrupted the BBB. Furthermore, the concurrent oral RO extract alleviated these conditions and repaired BBB by increasing the occludin expression and ameliorating structural changes in brain tissues. Consequently, the current data provide evidence that RO supplementation during IONP administration holds promise to minimize potential health risks, which should be corroborated by translational studies.

1. Introduction

Global scientific community interest has been piqued by the topic of nanotechnology. Many kinds of nanoparticles have been developed as a result of the notable acceleration of nanotechnology development [42]. Iron oxide nanoparticles (IONPs) have been widely synthesized for many applications because of their remarkable magnetic characteristics, high water solubility, stability, and high surface-to-volume ratio [65].

IONPs have been applied in many fields including the biomedical, industrial, agricultural, and water treatment systems fields. IONPs are mostly used in biomedicine, particularly in the areas of magnetic resonance imaging, tissue healing, magnetic hyperthermia, gene therapy, and tumor localization [19,48,68]. The FDA has authorized them for several uses, including the treatment of iron deficiency anemia and as contrast agents for imaging liver lesions and lymph node metastases [45].

Abbreviations: IONPs, iron oxide nanoparticles; RO, rosemary; TNF- α , tumor necrosis factor- α ; PARP-1, poly ADP-ribose polymerase; AIF, apoptosis-inducing factor; NF- κ B, nuclear factor-kappa B; α -s, α -synuclein; β -APP, beta- Amyloid protein precursor; TDP-43, TAR DNA binding protein of 43; BBB, blood brain barrier; MDA, malondialdehyde; NO, nitric oxide; GSh, educed glutathione.

* Corresponding author.

E-mail address: emy.khayal@yahoo.com (E.E.-S. Khayal).

<https://doi.org/10.1016/j.toxrep.2025.101935>

Received 17 October 2024; Received in revised form 18 January 2025; Accepted 28 January 2025

Available online 31 January 2025

2214-7500/© 2025 The Author(s). Published by Elsevier B.V. This is an open access article under the CC BY-NC-ND license (<http://creativecommons.org/licenses/by-nc-nd/4.0/>).

IONPs have to be directly injected into the human body for these medicinal uses, raising worries about potential harmful effects [18]. In addition to these uses, widespread usage of IONPs in the textile and cosmetics sectors causes an accumulation of the material that poses a risk to human health, making it an attractive subject for study [8].

The generation of reactive oxygen species (ROS) and the development of oxidative stress are two of the most commonly proposed mechanisms underlying the toxicity of nanomaterials. These processes lead to the induction of an inflammatory response by modulating intracellular calcium concentrations, triggering transcription factors, and inducing the production of cytokines [6]. Oxidative stress and inflammation cause damage to biomolecules such as proteins, lipids, and DNA. This contributes to cell and tissue damage, which can result in cytotoxic, fibrotic, and genotoxic reactions that are linked to illness [36].

The brain is more vulnerable to oxidative stress due to the decreased activity of enzymes that eliminate free radicals, such as glutathione peroxidase (GPx), catalase (CAT), and Superoxide dismutase (SOD), [12]. IONPs can reach the brain through the blood-brain-barrier (BBB) following systemic administration, the olfactory nerve following ingestion or inhalation, or they can enter the brain directly by intracerebral delivery [20]. While some research indicates that IONPs are biocompatible and low in toxicity, other research demonstrates that the application of IONPs can have hazardous consequences by producing ROS as a result of the Fenton reaction [32,64].

Ancient remedies made use of natural products and herbal medications. Due to their low risk of side effects and problems, herbs have garnered increased attention from researchers in recent decades as potential new drugs. Worldwide medical and pharmaceutical research has been rising in response to the growing need [11].

Folk medicine has utilized rosemary, *Rosmarinus officinalis* L. (*Labiatae*) (RO), to treat a variety of illnesses, such as headache, menstrual cramps stomachache, seizures, rheumatic pain, spasms, nervous anxiety, memory improvement, hysteria, depression, physical and mental exhaustion [21]. The vast spectrum of therapeutic effects of rosemary and its components, including anti-inflammatory, antioxidant, antinociceptive, neuroprotective, antidepressant, anti-hysterical, and ameliorative of memory and mental tiredness, is shown by several types of research conducted either on animal models or on cultured cells [57].

Rosemary extract (RO) is widely recognized for its antioxidant properties, which are primarily attributed to its high content of phenolic compounds such as carnosic acid and rosmarinic acid. These compounds play a crucial role in alleviating ROS by scavenging free radicals, reducing oxidative stress, and modulating the activity of antioxidant enzymes like SOD, CAT, and GPx [40] or key signaling of pro-inflammatory and inflammatory pathways [24]. The present work set out to estimate the potential protective role of the orally administered extract of RO against the toxic effects of injected IONPs on the brain tissues of adult male albino rats. It aimed to explore the potential underlying mechanisms involved in reversing such toxicity.

2. Materials and methods

2.1. Chemicals

Iron oxide nanoparticles (Fe_2O_3) (IONPs) were obtained from Sigma-Aldrich (Louis, Mo, USA), (Cas N. 900042). It was a brownish liquid, and sterile saline was used as a vehicle.

The chemicals of extraction and distilled water were obtained from the Forensic and Clinical Toxicology Research Laboratory, Faculty of Medicine, Zagazig University, Egypt.

2.2. Characterization of IONPs (Fe_2O_3)

The size and morphology of the IONPs were investigated by dropping an aqueous dispersion of the NPs onto a carbon-coated copper grid and

drying it in the open air. The Electron Microscope Unit at the Faculty of Agriculture, Al-Mansoura University in Egypt, used transmission electron microscopy (TEM) for characterization.

2.3. Plant and extract preparation

Fresh Rosemary (*Rosmarinus officinalis* L.) (RO) plant was obtained from the Faculty of Agricultural, Zagazig University, Egypt. The whole plant of RO, excluding its flowers, was used. To eliminate any dust or residual particles, the samples underwent cleaning and were rinsed with distilled water. Subsequently, they were air-dried for one week in a dark, air-conditioned room at 25 °C and then were ground in the milling machine. 100 g of the resultant powder was soaked in 1000 mL of (30:70) methanol at 60 °C for 1 h.

The mixture was filtered and evaporated under a vacuum rotary apparatus. The extract was dried in an incubator at reduced pressure and 40 °C and stored in a freezer at -4 °C to be used later [5].

2.4. Gas chromatography-mass spectrometry (GC-MS) analysis

To determine the chemical composition of the methanolic extract of *Rosmarinus officinalis* L., the extract was subjected to GC-MS analysis. The analysis was done using a gas chromatograph (Model: GC-MS (ISQ LT trace 1300), Thermo Fisher Scientific S.p.A. Milan, Italy. S.N. 420131158). The qualitative analysis was described by Ojeda-Sana et al. [53].

The injection technique was split mode. The capillary column was 30 m in length, with an inner diameter of 0.25 mm, and coated with a 0.25-TG-5MS stationary phase. The carrier gas was Helium with a flow rate of 1.87 mL/min. The initial column temperature was programmed at 90 °C for 5 min, then increased at a rate of 3 °C/min at 230 °C and held for 13 min. The injector temperature was adjusted to 255 °C. The constituents of the extract were thoroughly identified by matching their mass spectral fragmentation patterns with those documented in computerized MS data bank spectral libraries.

2.5. Animals and study design

Thirty adult male albino rats (Sprague Dawley) (*Rattus norvegicus*) weighing 200–220 g, were procured from the animal facility at the Faculty of Veterinary Medicine, Zagazig University. They underwent a seven-day acclimatization period in laboratory conditions before the commencement of the experiment. The rats were housed in sanitary cages maintained at temperatures between 22 and 25 °C, with 60 % humidity, and subjected to a 12-h light/12-h dark cycle. They had ad libitum access to food and water. The research adhered to international standards for animal studies, following the guidelines set forth by (the Guide for the Care and Use of Laboratory Animals) of the National Research Council [51] and ARRIVE guidelines (<https://arriveguidelines.org>). Meanwhile, the study is approved by the Institutional Animal Care and Use Committee (IACUC) at Zagazig University, Egypt (approval number: ZU-IACUC/3/F/97/2024).

The animals were randomly divided into five groups, each consisting of six rats.

- I. Control group: the rats received an essential diet and water for four weeks.
- II. Vehicle group: the rats were injected with 1 mL of sterile saline (IONPs solvent) intravenously through the caudal vein once a week for four weeks.
- III. Rosemary (RO) extract group: each rat received 1 mL of 100 mg/kg dissolved in saline by oral gavage needle [50] once a day for four weeks.
- IV. IONPs group: the rats were injected with 30 mg/kg of IONPs intravenously through the caudal vein once a week for four weeks [20].

V. IONPs and RO extract group: the rats received 100 mg/kg of the RO extract via oral gavage 1 h before IONPs injection once a day for four weeks followed by IONPs (30 mg/kg) administered by intravenous injection once a week for four weeks.

The weight of the animals was monitored weekly for dose adjustment. Twenty-four hs after the final dosing day, all rats had fasted overnight. They were anesthetized via intraperitoneal injection of pentobarbital at a dosage of 50 mg/kg. Decapitation was performed after confirming death. The brain of each rat was promptly dissected and rinsed with 0.9 % normal saline. The frontal cortex, a distinct brain subregion, was meticulously micro-dissected and systematically partitioned into three sections. The first stion was allocated for biochemical analyses, the second was preserved at -80°C for subsequent mRNA extraction, and the third was perfused with saline and fixed in 10 % neutral buffered formalin for histopathological and immunohistochemical investigations.

2.6. Biochemical analysis of brain tissues

A portion of brain tissue underwent wet digestion with 4 mL of concentrated nitric acid following the method outlined by Prohaska and Gybina, [55]. The iron content assay was conducted using both the Atomic Absorption Spectrophotometer (AAS) (Buck Scientific 210VGP Atomic Absorption Spectrophotometer) and a Perkin Elmer model (SpectraAA10, USA) flame atomic absorption spectrometer with a computer system. The data obtained were expressed as $\mu\text{g/g}$ wet weight.

The other part of the brain tissue was homogenized in phosphate-buffered saline and then centrifuged for 10 min. Subsequently, it was assessed colorimetrically for the estimation of malondialdehyde (MDA) according to the method described by Janero [33], reduced glutathione (GSH) using the method by Tietze [63], and nitric oxide (NO) contents following the procedure outlined by Grandati et al. [23]. Tumor necrosis factor- α (TNF- α) was determined using enzyme-linked immunosorbent assay rat ELISA analytical kits. The kits for these analyses were obtained from Biodiagnostic Co. (Giza, Egypt).

2.7. RT-qPCR analysis

The RNA isolation mini kit (RN easy, Qiagen Ltd, Germany) was used for the isolation of total ribonucleic acid (RNA) from brain tissue homogenates. Subsequently, the RNA was quantified and converted into complementary DNA (cDNA) using a Quantiscript reverse transcriptase kit (Quantitect Reverse Transcription kit, Qiagen, Germany). The expression of mRNA was achieved using a reaction mixture containing SYBR Green Real-time PCR Master Mix. The PCR mixture was run on the Strata gene Mx3000P (Agilent Technologies, Santa Clara, CA, USA) following the manufacturer's instructions.

The primer pairs for poly ADP-ribose polymerase 1(PARP-1), apoptosis-inducing factor (AIF), nuclear factor kappa-light-chain-enhancer of activated B cells (NF- κ B), α -synuclein (α -S), β Amyloid protein precursor (β -APP), TAR DNA binding protein of 43 kDa (TDP-43), and the reference control gene; glyceraldehyde-3-phosphate dehydrogenase (GAPDH) were designed by National Center for Biotechnology Information (NCBI) at <https://www.ncbi.nlm.nih.gov>. The Primer specificity was evaluated using the BLAST program(<http://blast.ncbi.nlm.nih.gov>). Table 1 displays the primer sequences and PCR conditions. The sequences of the used rat primers were purchased from (Bio-Diagnostics Egypt). The acquired amplification results were measured by the $2^{-\Delta\Delta\text{Ct}}$ method [41].

2.8. Histopathological examination of brain tissues

The brain tissues of each rat were placed in 10 % formaldehyde and dehydrated using ethanol in ascending series of concentrations, cleared in xylene and embedded in paraffin. Brain sections were prepared at

Table 1
primer sequences and RT-PCR conditions.

Gene	Primer sequences	PCR condition
PARP-1	Forward 5'-TAC CAT CTG GAG AGT CCG CA-3' Reverse 3'-ACA CGA CTC GAA CAT TGG CT-5'	95 °C-45s/60 °C-30 s/72 °C-60 s (40 cycles)
AIF	Forward 5'- AGC AAT GGC GTG TTC CTC TA-3' Reverse 3'- CCG GAT GGA TCT AGC TGC TG-5'	95 °C-10s/60 °C-20 s/72 °C-40 s (40 cycles)
NF- κ B	Forward 5'- ACG ATG GGA CGA CAC CTC TA-3' Reverse 3'-CGG AGC TCA TCT ATG TGC TGT CT-5'	95 °C-10 s/60 °C-30 s/72 °C-15 s (40 cycles)
α -S	Forward 5'- AGT TCT GCG GAA GCC TAG AG -3' Reverse 3'- AAC TGA GCA CTT GTA CGC CA -5'	94 °C-30 s/65 °C-30 s/68 °C-30 s (28cycles)
β -APP	Forward 5'-GCT TTA TAT ATG GCG GCT GCG G-3' Reverse 3'- CCG GCT GAG TGT CTT CGT TC -5'	95 °C-15 s/56 °C-30 s/72 °C-30 s (45 cycles)
TDP-43	Forward 5'-GAT CCT TCG TTG TGC TTC CTA GC-3' Reverse 3'- GGT TAT TTC CCA AGC CAG CTC -5'	95 °C-5 s/60 °C-30 s/72 °C-30 s (40 cycles)
GAPDH	Forward 5'- GAC TCT ACC CAC GGC AAG TT-3' Reverse 3'- GAT GGC ATG GAC TGT GGT CA -5'	94 °C-10 s/61 °C-30 s/72 °C-30 s (38 cycle)

PARP-1: poly ADP-ribose polymerase, AIF: apoptosis-inducing factor, NF- κ B: nuclear factor-kappa B, α -s: α -synuclein, β -APP: beta-Amyloid protein precursor, TDP-43: TAR DNA binding protein of 43 kDa.

5 μm thicknesses and stained with the routine hematoxylin and eosin technique [9].

2.9. Immunohistochemical staining for occludin

The immunohistochemistry technique was carried out using the Streptavidin-biotin method [28]. 4 μm thick brain sections were cut from the paraffin blocks and fixed on positively charged slides. The slides were then incubated for 30 min at 65 °C. Deparaffinization of all sections was performed using xylene. Following this, the sections were rehydrated and immersed in an EDTA buffer. The slides were placed in the microwave for antigen retrieval, adding hydrogen peroxide in methanol to antagonize endogenous peroxidase activity, and then incubating with 1 % bovine serum albumin [3]. All samples were incubated with Invitrogen™ Bioscience™ IHC Blocking Buffer (#00-4953-54) to block nonspecific binding sites of endogenous enzymes and antibodies.

This step minimized background staining and reduced false positives. Additionally, endogenous avidin and biotin were blocked by treating the samples with the Avidin/Biotin Blocking Kit (#004303) following the protocol by Alabiad et al. [4]. Sections were treated overnight at 4 °C with rabbit polyclonal antibody occludin (ab216327) primary antibodies (diluted 1: 200) [59]. The sections were rinsed with phosphate-buffered saline and then treated with the corresponding secondary antibody for 2 hs. Subsequently, the avidin-biotin complex (Abcam) was applied to the sections for 20 min. Staining was visualized using diaminobenzidine. Sections were counterstained with hematoxylin and observed under a light microscope.

2.10. Statistical analysis

The statistical data analysis was conducted using SPSS 26.0 software (IBM, Chicago, IL, USA) and GraphPad Prism 10 Software (Boston, Massachusetts USA). The Shapiro-Wilk Test was used to assess the normality of each variable One-way analysis of variance (ANOVA) and

the post hoc least significant difference test (LSD test) were performed and were presented as mean and standard deviation. A p -value of < 0.05 was considered to be statistically significant.

3. Results

3.1. IONPs characterization

TEM analysis of the IONPs revealed almost spherical particles ranging in size from 18 to 30.4 nm (Fig. 1).

3.2. GC-MS analysis of *Rosmarinus officinalis* L. extract

Fig. 2 displayed a chromatogram of the *Rosmarinus officinalis* L. methanolic extract. GC-MS analysis of the methanolic extract of *Rosmarinus officinalis* L. revealed several compounds, with the highest area percent including eucalyptol (29.56) at a retention time (11.87), Bicyclo [2.2.1]heptan-2-one,1,7,7-trimethyl-, (1 R)- (camphor) (16.32) at a retention time (15.24), borneol and its related metabolites (7.01) at retention time (15.85), and Caryophyllene (3.59) at a retention time (22.97) (Table 2).

3.3. IONPs-induced oxidative stress and inflammatory changes in brain tissues

Regarding brain tissue analysis for iron content, MDA, GSH, NO, and TNF- α , there were no significant differences between the control, vehicle, and RO extract groups, so we used the control group for comparison with other groups ($p > 0.05$) (Table 3). By using the ANOVA test, Table 4 showed significant differences between the control group, IONPs group, and IONPs and RO extract group respecting to iron content, MDA, GSH, NO, and TNF- α mean values in brain tissue homogenates ($p < 0.001$).

When IONPs (30 mg/kg) were injected intravenously once a week for four weeks, the mean values of iron content, MDA, NO, and TNF- α were significantly elevated while the mean values of GSH were significantly decreased when compared to the control group ($p < 0.001$) (Table 4). For four weeks the concurrent IV administration of IONPs with oral administration of 100 mg/kg RO extract once daily to the rats resulted in significant protection against the decline in GSH ($p < 0.001$) and significantly reduced the elevations in iron content ($p < 0.05$), MDA ($p < 0.05$), NO ($p < 0.05$), and TNF- α ($p < 0.001$) brought on by the IONPs administration (Table 4).

On comparing the IONPs and RO extract group with the control group, there were significant elevations in the mean values of iron content, MDA, NO, and TNF- α with significant decreases in the mean

values of GSH in the IONPs and RO extract group ($p < 0.001$) (Table 4).

3.4. IONPs-induced parthanatos in brain tissues

To determine whether parthanatos plays a role in IONPs-induced brain tissue cell death, the expression of genes specific to the parthanatos pathway was analyzed using RT-PCR. Fig. 3 shows a significant upregulation of PARP1 and AIF gene expressions, along with the increase of NF- κ B gene expression in brain tissues of the IONPs exposed group compared to the control, vehicle, and RO extract groups ($P < 0.001$).

Furthermore, concurrent administration of oral RO extract with IONPs resulted in a significant downregulation of PARP1, AIF, and NF- κ B gene expressions compared to the IONPs group ($P < 0.001$). When comparing the results of the RO extract +IONPs group with control, vehicle, and RO extract groups, significant differences were still observed in terms of PARP1 and AIF gene expressions. However, no-significant difference was observed for NF- κ B gene expression ($P \geq 0.05$) (Fig. 3).

3.5. IONPs-induced neurodegenerative changes

The effect of IONPs on neurodegenerative changes-related genes was investigated by examining the expression of α -S, β -APP, and TDP-43 genes. The IONPs exposed group showed a significant upregulation of α -S, β -APP, and TDP-43 gene expressions in the brain tissues of rats compared to the control, vehicle, and RO extract groups ($p < 0.001$) (Fig. 4).

Moreover, the concurrent administration of oral RO extract with the IONPs resulted in a significant downregulation of α -S, β -APP, and TDP-43 gene expressions compared to the IONPs group ($P < 0.001$). Additionally, significant differences were also observed when compared to control, vehicle, and RO extract groups ($p < 0.001$) (Fig. 4).

3.6. Histopathological examination of brain tissues

The Hematoxyline and Eosin stain for histopathological examination of brain tissues from control, vehicle, and RO extract groups revealed normal tissue structure with normal neurons (Fig. 5. A, B, and C). In contrast, brain sections of the IONPs exposed group exhibited vacuolation, degeneration, and apoptotic bodies in neuronal cells, along with dilated blood vessels and blood extravasation (Fig. 5. D and E). However, the oral RO extract+IONPs group showed improvement in the neuronal changes with only mild vacuolation, and no apoptotic bodies were observed (Fig. 5. F).

3.7. Immunohistochemical staining of brain tissues

The immunohistochemical examination of brain tissues for occludin expression revealed that the control, vehicle, and RO extract groups showed a strong immune-positive reaction of occludin protein expression (Fig. 6. A, B, and C). The IONPs exposed group showed an immune-negative reaction of occludin protein (Fig. 6. D). Moreover, the RO extract+IONPs group showed an immune-positive reaction with higher expressed occludin protein (Fig. 6. E).

The morphometric analysis revealed a significant reduction in the area percentage of occludin in the IONPs group versus the control, vehicle, and RO extract groups ($p < 0.0001$). On the contrary, the RO extract+IONPs group exhibited a significantly increased area percentage of occludin compared to the IONPs group ($p < 0.0001$) and a non-significant difference compared to the control, vehicle, and RO extract groups ($p > 0.05$) (Fig. 6. F).

4. Discussion

The ability of IONPs to cross the blood-brain barrier (BBB) facilitates

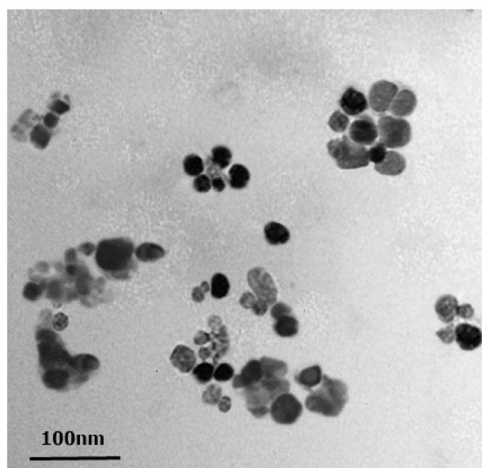


Fig. 1. Transmission electron microscopy image of IONPs.

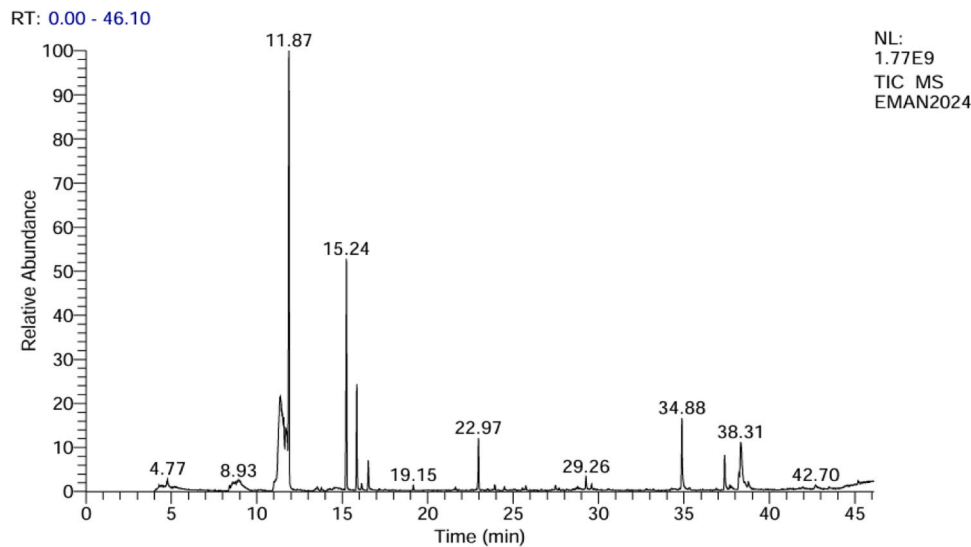


Fig. 2. GC-MS chromatogram of Rosmarinus officinalis L. methanolic extract.

Table 2

GC-MS Chemical composition of Rosmarinus officinalis L. methanolic extract.

Rt	Name	Molecular formula	Molecular weight	Area percent
11.36	Eucalyptol (1,8-cineole)	C10H18O	154	19.73
11.57	Eucalyptol (1,8-cineole)	C10H18O	154	2.23
11.75	Eucalyptol (1,8-cineole)	C10H18O	154	4.48
11.87	Eucalyptol (1,8-cineole)	C10H18O	154	29.56
15.24	Bicyclo[2.2.1]heptan-2-one,1,7,7-trimethyl-, (1R)- (Camphor)	C10H16O	152	16.32
15.85	Bicyclo[2.2.1]heptan-2-ol,1,7,7-trimethyl-, (1S-endo)-	C10H18O	154	7.01
	Isoborneol	C10H18O	154	
	Borneol	C10H18O	154	
16.52	3-Cyclohexene-1-methanol, 4,4-trimethyl- (α -terpinenol)	C10H18O	154	2.09
	p-menth-1-en-8-ol	C10H18O	154	
22.97	Caryophyllene	C15H24	204	3.59
	Bicyclo[7.2.0]undec-4-ene,4,11,11-trimethyl-8-methylene-, [1R-(1R*,4Z,9S*)]-	C15H24	204	
29.26	Caryophyllene oxide	C15H24O	220	0.96
	trans-Z- β -Bisabolene epoxide	C15H24O	220	
34.88	Hexadecanoic acid, methyl ester	C17H34O2	270	5.07
37.38	Ethanone,1-(1,2,3,5,6,7-hexahydro-1,1,5,5-tetramethyl-s-indacen-4-yl)-	C18H24O	256	2.62
	Azulen-2-ol,1,4-dimethyl-7-(1-methylethyl)-	C15H18O	214	
	1H-Indene, 2-butyl-3-hexyl-	C19H28	256	
38.21	9,12-Octadecadienoic acid, methyl ester, (E,E)-	C19H34O2	294	1.02
38.32	10-Octadecenoic acid, methyl ester	C19H36O2	296	5.33
	11-Octadecenoic acid, methyl ester	C19H36O2	296	
	8-Octadecenoic acid, methyl ester	C19H36O2	296	

Rt: retention time

Table 3

Comparison of mean values of iron content, malondialdehyde (MDA), glutathione (GSH), nitric oxide (NO), and tumor necrosis factor α (TNF- α) in brain tissues among control, vehicle, and rosemary (RO) extract groups by ANOVA test.

Parameter	Control group	Vehicle group	RO extract group	F	P
Iron content ($\mu\text{g/g}$)	16.37 \pm 0.54	16.20 \pm 0.43	16.43 \pm 0.43	0.367	0.69
MDA (nmol/mg)	3.39 \pm 0.28	3.34 \pm 0.14	3.40 \pm 0.20	0.879	0.13
GSH (nmol/g)	1.39 \pm .04	1.3900 \pm .02280	1.3817 \pm .04021	0.890	0.12
NO ($\mu\text{mol/mg}$)	1.67 \pm .05	1.66 \pm 0.06	1.65 \pm 0.04	0.802	0.22
TNF- α (pg/mg)	56.62 \pm 2.19	58.68 \pm 2.69	59.32 \pm 0.45	2.943	0.08

Values are presented as the mean \pm standard deviation (SD), n = 6. F test: ANOVA test

Table 4

Comparison of mean values of iron content, malondialdehyde (MDA), reduced glutathione (GSH), nitric oxide (NO), and tumor necrosis factor α (TNF- α) in brain tissues among control, IONPs, and IONPs + rosemary (RO) extract groups by ANOVA and LSD tests.

Parameter	Control group	IONPs group	IONPs + RO extract group	F	P
Iron content ($\mu\text{g/g}$)	16.37 \pm 0.54	23.33 \pm 0.73 ^a	22.12 \pm 0.56 ^{ab}	219.41	0.000
MDA (nmol/mg)	3.39 \pm 0.28	7.42 \pm 0.59 ^b	6.31 \pm 0.57	102.92	0.000
GSH (nmol/g)	1.39 \pm .04	0.82 \pm 0.03 ^b	1.12 \pm 0.11 ^{a c}	97.13	0.000
NO ($\mu\text{mol/mg}$)	1.67 \pm 0.05	2.05 \pm 0.11 ^a	1.93 \pm 0.07	34.01	0.000
TNF- α (pg/mg)	58.92 \pm 2.19	76.63 \pm 3.05 ^a	70.48 \pm 1.49 ^{b c}	115.92	0.000

Values are presented as the mean \pm standard deviation (SD), n = 6. F test: ANOVA test, IONPs: iron oxide nanoparticles

By least significance test (LSD):

^a : p < 0.001 in comparison to the control group.

^b : p < 0.05 in comparison to the IONPs group; ^c : p < 0.001 in comparison to the IONPs group

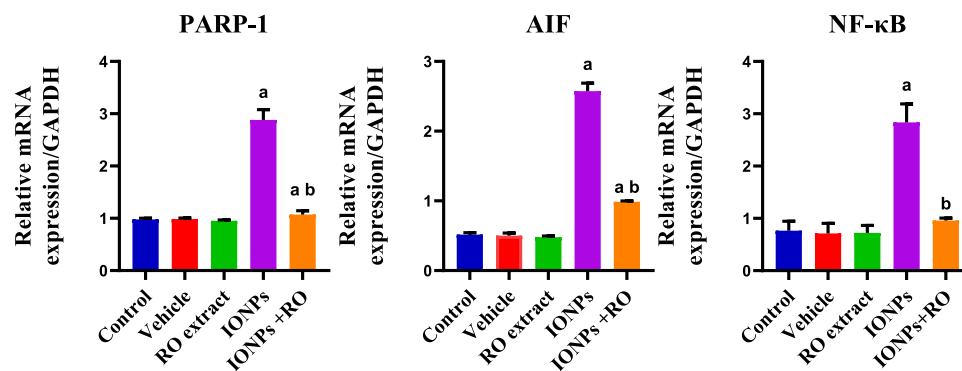


Fig. 3. Effects of IONPs on parthanatos pathway-specific genes (PARP1, AIF, NF-κB) expression. mRNA expression was assessed by RT-PCR. Data are the mean \pm standard deviation (SD), $n = 6$. [a: Highly significant difference as compared to the control group ($p < 0.01$), b: Highly significant difference as compared to the IONPs group ($p < 0.01$).

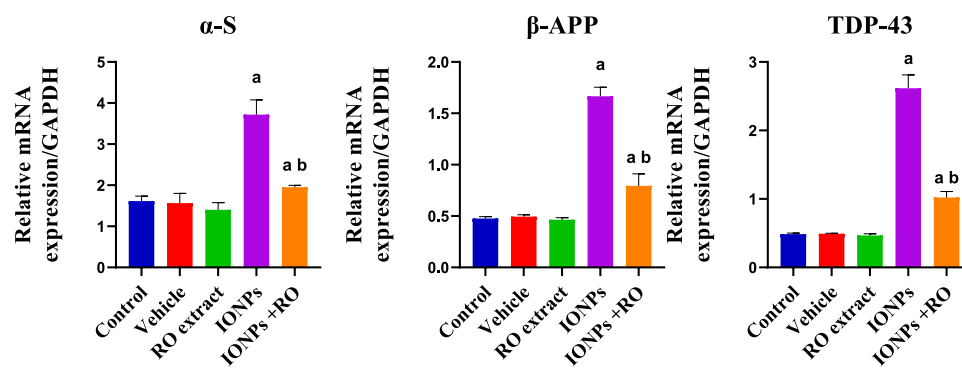


Fig. 4. Effects of IONPs on neurodegenerative changes-related genes (α -S, β -APP, TDP-43) expression. mRNA expression was assessed by RT-PCR. Data are the mean \pm standard deviation (SD), $n = 6$. [a: Highly significant difference as compared to the control group ($p < 0.001$), b: Highly significant difference as compared to the IONPs group ($p < 0.001$)].

their application in CNS diagnostic measures and therapies, ranging from microglial cell modulation to improved magnetic resonance imaging (MRI) contrast and drug delivery systems [52].

Rosmarinus officinalis L. (rosemary) has long been used in traditional medicine for neurological conditions such as memory disorders, depression, and mental health issues. Its therapeutic benefits are attributed to its antimicrobial, antioxidant, anti-inflammatory, and anti-apoptotic properties, which help activate antioxidant enzymes and reduce free radicals, offering protection against oxidative stress-related diseases [21].

Therefore, the present study investigated the potential protective role of the methanolic extract of RO against IONPs-induced brain toxicity in adult rats over 4-weeks and explored the potential underlying mechanisms involved in reversing such toxicity.

In the current study, GC-MS analysis of the methanolic RO extract revealed eucalyptol as the predominant compound, consistent with Alhailoul et al. [5]. Eucalyptol, a key component of various essential oils, including rosemary, is known for its anti-inflammatory, antioxidant, bronchodilatory, and antimicrobial effects, supporting its traditional medicinal use [27].

The biochemical analysis of the present study demonstrated that IONPs increased brain iron levels, MDA, NO, and TNF- α while decreasing GSH levels, consistent with previous findings [13,14,16]. These studies confirm that IONPs can cross the BBB by upregulating brain iron receptors via iron/transferrin binding [58]. Once inside the brain, IONPs induce oxidative stress through the Fenton reaction, leading to elevated MDA levels, a marker of lipid peroxidation, and impairing mitochondrial function, which contributes to neurodegenerative disorders [62]. The resulting iron accumulation further depletes GSH levels, weakening the brain's antioxidant defenses [70].

Additionally, IONPs elevate NO and TNF- α levels in brain tissues suggesting nitrosative stress-induced DNA damage [31] and neuro-inflammation, consistent with the pro-inflammatory effects of IONPs and its role in promoting neuronal death and contributing to neurodegenerative diseases [10].

RO extract ameliorated these changes, reducing iron levels, MDA, and NO while restoring GSH and decreasing TNF- α . These protective effects are consistent with the well-documented antioxidant and anti-inflammatory properties of RO [1,21,66] and the ROS-scavenging and NF- κ B inhibition activities of eucalyptol [22,27]. These effects are attributed to eucalyptol, which enhances antioxidant activity by scavenging ROS and chelation of metal ions [27], while its anti-inflammatory effect is mediated through NF- κ B inhibition, resulting in reduced production of NO and TNF- α [22].

Recent studies highlight emerging cell death mechanisms like parthanatos. This study investigated whether IONPs are implicated in such a mechanism of cell death induction as well as examining the protective role of RO extract.

The Molecular results of the current study demonstrated that repeated IONPs exposure for 4 weeks increased gene expression of PARP-1, AIF, and NF- κ B. No previous studies have discussed parthanatos as a potential mechanism of IONPs-induced toxicity. However, our results are consistent with a previous study that reported increased PARP-1 and cleaved caspase-3 expression in brain regions of IONPs intoxicated mice [13].

Parthanatos, a caspase-independent cell death pathway, is triggered by PARP-1 overactivation due to DNA damage caused by factors like NO production, ROS generation, and radiation exposure. This leads to PAR polymer accumulation, mitochondrial depolarization, AIF release, and nuclear translocation, resulting in DNA fragmentation and cell death

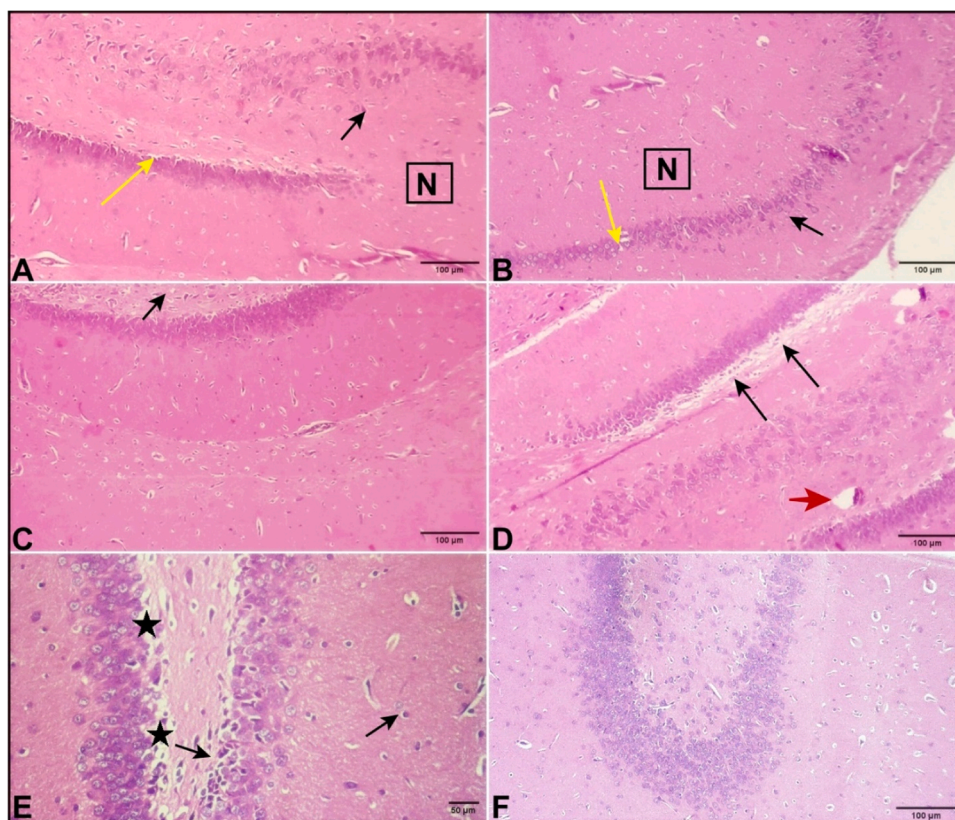


Fig. 5. Photomicrographs of the brain tissue sections of studied groups; (A) The control group displayed normal brain tissue with normal neurons (N), normal astrocytes (black arrow), and granular layer (yellow arrow) (H&E, x200). (B) the vehicle group showed a section of brain tissue containing normal pyramidal cells with a normal nucleus (black arrow) and normal neuron (N) (H&E, x200). (C) the RO extract group showed a section of the brain with normal pyramidal cells (black arrow) (H&E, x200). (D) IONPs group showed a section of brain tissues with vacuolation (black arrow), dilated blood vessels and extravasated blood cells (red arrow) (H&E, x200). (E) IONPs group showing degeneration and vacuolization of the neuronal cells (star) and apoptotic bodies (black arrow) (H&E, x400). (F) brain tissue section of the RO extract + IONPs group showed improvement of the neuronal changes with mild vacuolation and no apoptotic bodies (H&E, x200). RO: rosemary. IONPs: iron oxide nanoparticles.

[29,49].

PARP-1, a DNA-binding protein, is the most essential step in initiating parthanatos, consuming NAD and ATP during overactivation, causing ATP depletion and structural, functional cellular changes, and eventual cell death [29]. AIF, a mitochondrial flavoprotein critical for cell survival, becomes a mediator of parthanatos under stress, driving DNA fragmentation after its nuclear translocation [49]. Additionally, PARP-1 overactivation stimulates NF- κ B, a transcription factor, promoting inflammatory mediator expression [43].

Interestingly, RO extract reduced PARP-1 and AIF expression and restored NF- κ B levels to normal. This suggests that RO disrupts parthanatos. Previous studies have shown the protective role of RO extract through the reduction of NF- κ B expression [34,71] or by decreasing other inflammatory mediators [69]. While no studies have directly examined the role of RO extract in parthanatos-mediated cell death, its protective role was attributed to the effect of the eucalyptol ingredient, which restored the PARP protein activity [27].

Regarding the neurodegenerative effects of IONPs, the current study demonstrated upregulation of the gene expression of α -S, β -APP, and TDP-43 in brain tissues of the IONPs group. These results agree with those of Imam et al. [30], who reported increased α -S aggregation associated with IONPs toxicity and attributed this aggregation to IONPs-induced oxidative stress. Similarly, Sadeghi and Marefat [60] reported increased β -APP and A β expression in hippocampal cells after exposure to IONPs. They suggested that β -APP upregulation might be due to iron accumulation inside the cells, oxidative damage resulting from IONPs toxicity, or a synergistic effect of both factors.

The pathogenesis of neurodegenerative disorders, such as

Parkinson's disease and Alzheimer's disease, is marked by multiple features, including abnormal protein deposits in brain regions, such as α -S aggregates, non-amyloid components of APP, and ubiquitin [7]. Additionally, it encompasses neuroinflammation, metal ion dyshomeostasis (e.g., iron), oxidative stress, mitochondrial dysfunction, neurofibrillary tangles, A β plaques, synaptic toxicity, reduced brain metabolism, brain stress, and BBB dysfunction [47].

α -S aggregates, the hallmark of Parkinson's disease, form intracellular inclusions known as Lewy bodies, impairing ionic homeostasis, and synaptic transmission, leading to neuronal degeneration and death [7]. Similarly, the hydrolytic cleavage of β -APP results in the deposition of soluble A β oligomers, with the long-term accumulation and enhancement of A β plaques causing a loss of synaptic plasticity and toxicity [15]. Furthermore, The TDP-43, a nuclear protein and the main protein component of the ubiquitinated inclusions, forms cytoplasmic inclusions, leading to neuronal degeneration due to its nuclear depletion [35].

Interestingly, the RO extract reversed these changes, highlighting its neuroprotective role. This effect may be attributed to the inhibition of A β oligomerization, potentially facilitated by eucalyptol's lipophilic nature and ability to cross the BBB, protecting against iron-induced cell death [27], or by the action of RO's polyphenols and monoamines [25]. Additionally, RO enhances neuronal function by reducing β -APP levels in the hippocampus [39].

Regarding the histopathological and immunohistochemical examination of brain tissues of IONPs, the present study revealed apoptotic degeneration, vacuolization, and congestion of neuronal cells in the brain sections of the IONPs exposed group. Additionally, there was a

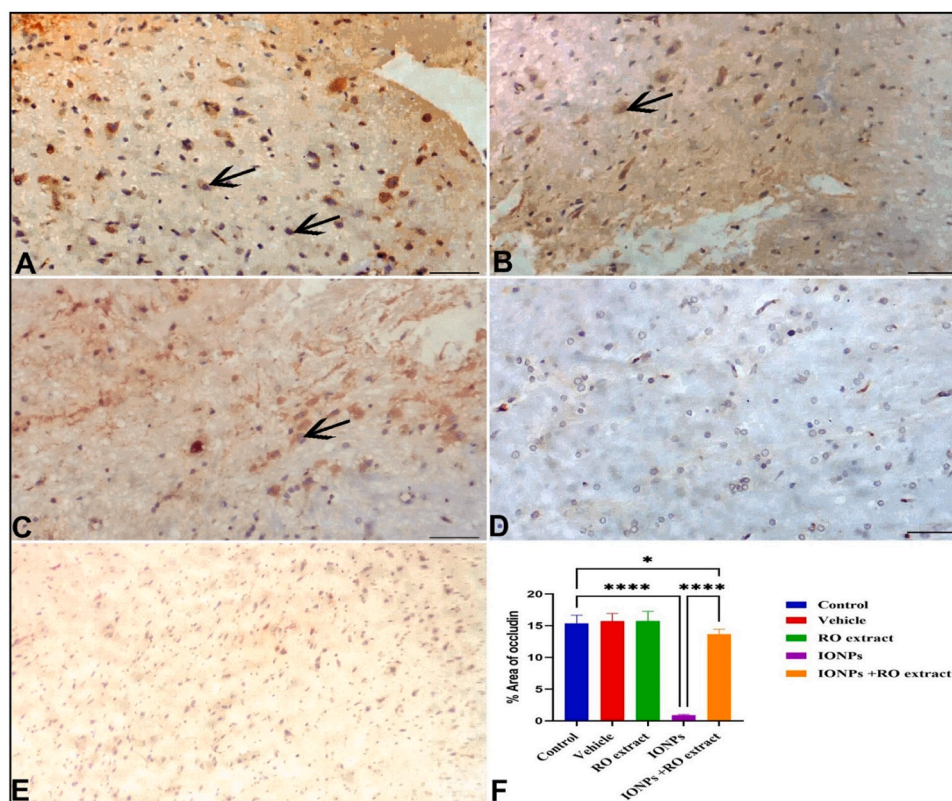


Fig. 6. Photomicrographs of immunohistochemical expression of occludin in the brain tissues of studied groups; (A) control group, (B) vehicle group, and (C) RO extract group showed normal brain tissue with positive staining, indicated by the presence of brown granules (arrows) of occludin expressing cells. (D) The IONPs group showed negative staining. (E) IONPs + RO extract group showed positive staining (occludin immunoreactivity x200). (F) A histogram demonstrating the area % of occludin. ***: $p < 0.0001$, *: $p > 0.05$. RO: Rosemary. IONPs: iron oxide nanoparticles.

negative immunostaining reaction, with decreased occludin expression in neuronal cells.

These findings are consistent with previous studies [14,38], which reported neuronal degeneration, cell death, congestion, and other IONPs induced structural changes in brain tissues [14]. These pathological findings are linked to elevated brain iron levels, as IONPs can penetrate the BBB more effectively, causing greater brain cell damage [56]. IONPs-induced oxidative stress alters cellular structures, while increased iron binding to transferrin upregulates brain iron receptors, enhancing iron transport across the BBB [2].

Occludin, a tight junction protein, is essential for BBB integrity, with higher expression in neuronal tissues making the BBB less permeable than other tissue barriers. BBB permeability is influenced by both the expression levels and distribution of occludin. Reduced occludin expression impairs BBB function, and elevated brain iron levels have been shown to decrease occludin, leading to BBB disruption and brain damage [72]. In this study, the increased brain iron levels in the IONPs-treated group may be linked to suppressed occludin expression.

The administration of RO extract with IONPs revealed improvement of neuronal degenerative changes, with only slight vacuolation observed. Additionally, there was a strong immune-positive reaction, with increased occludin expression in neuronal cells.

Previous studies have demonstrated the protective role of RO in restoring structural brain tissue damage caused by toxic agents, improving aging-related neuronal changes, and reducing BBB permeability in acute ischemic injury [17,46,61]. This study further hypothesizes that RO's lipophilic component, eucalyptol, contributes to repairing BBB disruption caused by IONPs-induced neurotoxicity.

The current study hypothesized a mechanistic cascade in which IONPs-induced oxidative and nitrosative stress triggers DNA damage, stimulating PARP-1 overactivation [26]. This overactivation elevates

TNF- α and upregulates NF- κ B in neuronal cells via a DNA damage-independent signaling pathway [54].

PARP-1-induced parthanatos contributes to neurodegenerative disorders by upregulating inflammatory mediators, including TNF- α and iNOS, exacerbating inflammation [43]. Additionally, overactivated PARP-1 interacts with SIRT6, impairing the non-amyloidogenic processing of β -APP [67], and producing PAR, which accelerates pathological α -S aggregation, leading to neuronal cell death [37]. Similarly, PARP-1 overactivation promotes TDP-43 cytosolic translocation and aggregation, driving cytotoxicity in neurodegenerative disorders [44].

These findings provide new insights into the interplay between neuro-oxidative stress, neuro-inflammation, and parthanatos-mediated neuronal cell death, which collectively lead to neurodegenerative changes, establishing IONPs as a potential risk factor for CNS toxicity.

5. Conclusion

The intravenous administration of IONPs induced neurotoxicity in adult male rats, triggering a cascade of events, including structural degenerative changes and elevated iron levels in brain tissues. This led to reduced occludin expression and disruption of BBB, further exacerbated by the ability of NPs to penetrate BBB. IONPs-induced oxidative and nitrosative stress, as evidenced by increased MDA and NO levels, alongside reduced GSH. Additionally, IONPs caused neuro-inflammation and parthanatos-mediated neuronal cell death by increasing TNF- α levels, PARP-1, AIF, and NF- κ B mRNA expression. These incidents contributed to neurodegenerative changes, reflected in increased mRNA expression of α -S, β -APP, and TDP-43.

Conversely, concurrent oral administration of RO extract alleviated these effects by limiting the iron accumulation in brain tissues, exhibiting antioxidant effects via decreased MDA and increased GSH levels.

Its anti-inflammatory properties were demonstrated through the reduction of TNF- α levels and NF- κ B mRNA expression. Additionally, RO extract showed a newly discovered ability to attenuate parthanatos-mediated neuronal cell death and repair the BBB, evidenced by increased occludin expression and reduced structural brain tissue damage.

Consequently, the current data suggest that RO supplementation during IONPs administration holds promise to minimize potential health risks, which should be corroborated by translational studies. Additionally, further studies are needed to fully elucidate and confirm the role of eucalyptol, as its potential effects require additional investigation to validate the hypothesis proposed in this study.

6. Limitations of the study

The study did not assess oxidative stress markers such as superoxide dismutase, catalase, glutathione peroxidase, glutathione S transferase, or superoxide. Instead, it focused on reduced GSH, as it is the most abundant antioxidant in all cellular compartments, and a positive feedback loop exists between iron accumulation, low GSH levels, and oxidative stress. The buildup of iron leads to a decrease in GSH levels, which in turn triggers oxidative stress.

Author Contributions Statement

All authors contributed equally in collecting data, performing the analysis, writing the manuscript, and revising and approving the final copy.

Funding

The current study hasn't received any fund from any organizations or institutions.

CRedit authorship contribution statement

Ahmed Mona Mostafa: Methodology, Investigation, Formal analysis. **Khayal Eman El-Sayed:** Writing – review & editing, Writing – original draft, Methodology, Investigation, Formal analysis, Data curation, Conceptualization. **Elsheikh Arwa A.:** Writing – review & editing, Writing – original draft, Supervision, Methodology, Investigation, Formal analysis. **Abd-Almotaleb Noha Ali:** Methodology, Investigation.

Declaration of Competing Interest

The authors declare that they have no known competing financial interests or personal relationships that could have appeared to influence the work reported in this paper.

Data availability

Data will be made available on request.

References

- [1] E. Abdelrazik, H.M. Hassan, E. Hamza, F.M. Ezz Elregal, M.H. Elnagdy, E. A. Abdulhai, Beneficial role of rosemary extract on oxidative stress-mediated neuronal apoptosis in rotenone-induced attention deficit hyperactivity disease in juvenile rat model, *Acta Biomed.* 94 (3) (2023) e2023104, <https://doi.org/10.23750/abm.v94i3.14260>.
- [2] R. Agarwal, S. Adhikary, S. Bhattacharya, Si Goswami, D. Roy, et al., Iron oxide nanoparticles: a narrative review of in-depth analysis from neuroprotection to neurodegeneration, *Environ. Sci. Adv.* 3 (5) (2024) 635–660, <https://doi.org/10.1039/d4va00062e>.
- [3] M.A. Alabiad, M.S. Elderey, A.M. Shalaby, Y. Nosery, M.A. Gobran, The usefulness of 4 immunoperoxidase stains applied to urinary cytology samples in the pathologic stage of urothelial carcinoma: a study with histologic correlation, *JAI Morphol.* 29 (6) (2021) 422–432, <https://doi.org/10.1097/PAL.0000000000000905>.
- [4] M.A. Alabiad, O.A. Harb, H.F. Taha, B.S. El Shafaay, L.M. Gertallah, N. Salama, Prognostic and clinic-pathological significances of SCF and COX-2 expression in inflammatory and malignant prostatic lesions, *JP Res. O* 25 (2) (2019) 611–624, <https://doi.org/10.1007/s12253-018-0534-1>.
- [5] H.A.S. Alhaithloul, M.M. Alqahtani, M.A. Abdein, M.A.I. Ahmed, A.E.-L. Hesham, M.M.E. Aljameeli, R.N. Al Mozini, F.N. Gharsan, S.M. Hussien, Y.A. El-Amier, Rosemary and neem methanolic extract: antioxidant, cytotoxic, and larvicidal activities supported by chemical composition and molecular docking simulations, *Front. Plant Sci.* 14 (2023) 1155698, <https://doi.org/10.3389/fpls.2023.1155698>.
- [6] A.A. Aljabali, M.A. Obeid, R.M. Bashatwah, A. Serrano-Aroca, et al., Nanomaterials and their impact on the immune system, *Int. J. Mol. Sci.* 24 (3) (2023) 2008, <https://doi.org/10.3390/ijms24032008>.
- [7] S. Amartumur, H. Nguyen, T. Huynh, et al., Neuropathogenesis-on-chips for neurodegenerative diseases, *Nat. Commun.* 15 (2024) 2219, <https://doi.org/10.1038/s41467-024-46554-8>.
- [8] M.O. Ansari, N. Parveen, M.F. Md Fahim Ahmad, A.L. Wani, S. Afrin, Y. Rahman, S. Jameel, Y.A. Khan, H.R. Siddique, M. Tabish, G.G.H.A. Shadab, Evaluation of DNA interaction, genotoxicity and oxidative stress induced by iron oxide nanoparticles both in vitro and in vivo: attenuation by thymoquinone, *Sci. Rep.* 9 (1) (2019) 6912, <https://doi.org/10.1038/s41598-019-43188-5>.
- [9] Bancroft J.D., Layton C. (2013) The hematoxylin and eosin. In: Theory & practice of histological techniques, Suvarna SK, Layton C, Bancroft JD. (Eds.) 7th Edition, Churchill Livingstone of El Sevier, Philadelphia, Ch. 10 and 11, 172-214. <https://doi.org/10.1016/B978-0-7020-4226-3.00010-X>.
- [10] A. Behera, N. Sa, S.P. Pradhan, S. Swain, P.K. Sahu, Metal Nanoparticles in Alzheimer's Disease, *J. Alzheimers Dis. Rep.* 7 (1) (2023) 791–810, <https://doi.org/10.3233/ADR-220112>.
- [11] A. Boyd, C. Bleakley, C. Gill, S. McDonough, D.A. Hurley, P. Bell, J.G. McVeigh, M. Hannon- Fletcher, Herbal medicinal products or preparations for neuropathic pain and fibromyalgia, *Cochane Database Syst. Rev.* 4 (4) (2019), <https://doi.org/10.1002/14651858.CD010528.pub4>.
- [12] S.B. Chidambaram, N. Anand, S.R. Varma, S. Ramamurthy, C. Vichitra, A. Sharma, A.M. Mahalakshmi, M.M. Essa, Superoxide dismutase and neurological disorders, *IBRO Neurosci. Rep.* 16 (2024) 373–394, <https://doi.org/10.1016/j.ibneur.2023.11.007>.
- [13] V. Dhakshinamoorthy, V. Manickam, E. Perumal, Neurobehavioural toxicity of iron oxide nanoparticles in mice, *Neurotox. Res.* 32 (2) (2017) 187–203, <https://doi.org/10.1007/s12640-017-9721-1>.
- [14] M.F. Dora, N.M. Taha, M.A. Lebda, A.E. Hashem, M.S. Elfeky, Y.S. El-Sayed, S. A. Jaouni, A.H. El-Far, Quercetin attenuates brain oxidative alterations induced by iron oxide nanoparticles in rats, *Int. J. Mol. Sci.* 22 (8) (2021) 3829, <https://doi.org/10.3390/ijms22083829>.
- [15] S.K. Dubey, K. Lakshmi, K.V. Krishna, M. Agrawal, SinghviG, R.N. Saha, S. Saraf, S. Saraf, R. Shukla, A. Alexander, Insulin mediated novel therapies for the treatment of Alzheimer's disease, *Life Sci.* 249 (2020) 117540, <https://doi.org/10.1016/j.lfs.2020.117540>.
- [16] E.H.K. El-Sayed, Z.A. Mohammed, M.M. Ahmed, Ameliorative role of quercetin in iron overload induced heart and brain toxicity in adult male albino rats, *J. Toxicol. Environ. Health Sci.* 11 (2) (2019) 16–26, <https://doi.org/10.5897/JTEHS2019.0429>.
- [17] M. Eslami Farsani, Sh Razavi, H. Rasoolijazi, E. Esfandirami, R. Seyedebrahimi, Sh Ababzadeh, Neuroprotective effects of rosemary extract on white matter of prefrontal cortex in old rats, *Iran. J. Basic Med. Sci.* 27 (2024) 518–523, <https://doi.org/10.22038/IJBMS.2023.74168.16117>.
- [18] U.S. Ezealigo, B.N. Ezealigo, S.O. Aisida, F.I. Ezema, Iron oxide nanoparticles in biological systems: antibacterial and toxicology perspective, *JCIS Open* 4 (2021) 100027, <https://doi.org/10.1016/j.jciso.2021.100027>.
- [19] H.M. Fahmy, O.A. Saad, M.M. Fathy, Insight into the photothermal therapeutic impacts of silica-coated iron oxide nanocomposites, *J. Drug Deliv. Sci. Technol.* 84 (2023) 104540, <https://doi.org/10.1016/j.jddst.2023.104540>.
- [20] U.S. Gaharwar, R. Meena, P. Rajamani, Biodistribution, clearance and morphological alterations of intravenously administered iron oxide nanoparticles in male wistar rats, *Int J. Nanomed.* 14 (2019) 9677–9692, <https://doi.org/10.2147/IJN.S223142>.
- [21] M.R. Ghasemzadeh, H. Hosseinzadeh, Therapeutic effects of rosemary (*Rosmarinus officinalis* L.) and its active constituents on nervous system disorders, *Iran. J. Basic Med. Sci.* 23 (9) (2020) 1100–1112, <https://doi.org/10.22038/ijbms.2020.45269.10541>.
- [22] C. Gonçalves, D. Fernandes, I. Silva, V. Mateus, Potential anti-inflammatory effect of rosmarinus officinalis in preclinical in vivo models of inflammation, *Molecules* 27 (3) (2022) 609, <https://doi.org/10.3390/molecules27030609>.
- [23] M. Grandati, C. Verrecchia, M.L. Revaud, M. Allix, R.G. Boulou, M. Plotkine, Calcium-independent NO-synthase ac-tivity and nitrites/nitrates production in transient focalcerebral ischemia in mice, *Br. J. Pharmacol.* 122 (4) (1997) 625–630, <https://doi.org/10.1038/sj.bjp.0701427>.
- [24] S. Habtemariam, Anti-inflammatory therapeutic mechanisms of natural products: insight from rosemary diterpenes, carnosic acid and carnosol, *Biomedicines* 11 (2) (2023) 545, <https://doi.org/10.3390/biomedicines11020545>.
- [25] T. Hase, S. Shishido, S. Yamamoto, R. Yamashita, H. Nukima, S. Taira, et al., Rosmarinic acid suppresses Alzheimer's disease development by reducing amyloid β aggregation by increasing monoamine serotonin, *Sci. Rep.* 9 (2019) 8711, <https://doi.org/10.1038/s41598-019-45168-1>.

- [26] C. Hegedűs, L. Virág, Inputs and outputs of poly (ADP-ribose) ation: relevance to oxidative stress, *Redox Biol.* 2 (2014) 978–982, <https://doi.org/10.1016/j.redox.2014.08.003>.
- [27] C.C. Hoch, J. Petry, L. Griesbaum, T. Weiser, K. Werner, M. Ploch, A. Verschoor, G. Multhoff, A. Bashiri Dezfouli, B. Wollenberg, 1,8-cineole (eucalyptol): a versatile phytochemical with therapeutic applications across multiple diseases, *Biomed. Pharmacother.* 167 (2023) 115467, <https://doi.org/10.1016/j.biopha.2023.115467>.
- [28] S.-M. Hsu, L. Raine, H. Fanger, Use of avidin-biotin-peroxidase complex (ABC) in immunoperoxidase techniques: a comparison between ABC and unlabeled antibody (PAP) procedures, *J. Histochem. Cytochem.* 29 (4) (1981) 577–580, <https://doi.org/10.1177/29.4.6166661>.
- [29] P. Huang, G. Chen, W. Jin, K. Mao, H. Wan, Y. He, Molecular mechanisms of parthanatos and its role in diverse diseases, *Int. J. Mol. Sci.* 23 (13) (2022) 7292, <https://doi.org/10.3390/ijms23137292>.
- [30] S.Z. Imam, Susan M. Lantz-McPeak, E. Cuevas, H. Rosas-Hernandez, S. Liachenko, Y. Zhang, S. Sarkar, J. Ramu, B.L. Robinson, Y. Jones, B. Gough, M.G. Paule, S. F. Ali, Z.K. Binienda, Iron oxide nanoparticles induce dopaminergic damage: in vitro pathways and in vivo imaging reveals mechanism of neuronal damage, *Mol. Neurobiol.* 52 (2) (2015) 913–926, <https://doi.org/10.1007/s12035-015-9259-2>.
- [31] O.M. Iova, G.E. Marin, I. Lazar, I. Stanescu, G. Dogaru, C.A. Nicula, A.E. Bulboacă, Nitric oxide/nitric oxide synthase system in the pathogenesis of neurodegenerative disorders-an overview, *Antioxidants* 12 (3) (2023) 753, <https://doi.org/10.3390/antiox12030753>.
- [32] E. Irrsack, S. Aydin, K. Bleckmann, et al., Local administrations of iron oxide nanoparticles in the prefrontal cortex and caudate putamen of rats do not compromise working memory and motor activity, *Neurotox. Res.* 42 (1) (2024) 6, <https://doi.org/10.1007/s12640-023-00684-x>.
- [33] D.R. Janero, Malondialdehyde and thiobarbituric acid-reactivity as diagnostic indices of lipid peroxidation and peroxidative tissue injury, *Free Radic Biol Med.* 9 (6) (1990) 515–540, [https://doi.org/10.1016/0891-5849\(90\)90131-2](https://doi.org/10.1016/0891-5849(90)90131-2).
- [34] B.R. Jin, K.S. Chung, S.Y. Cheon, M. Lee, S. Hwang, S.N. Hwang, K.J. Rhee, H.J. An, Rosmarinic acid suppresses colonic inflammation in dextran sulphate sodium (DSS)-induced mice via dual inhibition of NF- κ B and STAT3 activation, *Sci. Rep.* 7 (2017) 46252, <https://doi.org/10.1038/srep46252>.
- [35] M. Jo, S. Lee, Y.M. Jeon, S. Kim, Y. Kwon, H.J. Kim, The role of TDP-43 propagation in neurodegenerative diseases: integrating insights from clinical and experimental studies, *Exp. Mol. Med.* 52 (10) (2020) 1652–1662, <https://doi.org/10.1038/s12276-020-00513-7>.
- [36] K. Jomova, S.Y. Alomar, S.H. Alwasel, et al., Several lines of antioxidant defense against oxidative stress: antioxidant enzymes, nanomaterials with multiple enzyme-mimicking activities, and low-molecular-weight antioxidants, *Arch. Toxicol.* 98 (2024) 1323–1367, <https://doi.org/10.1007/s00204-024-03696-4>.
- [37] T.I. Kam, X. Mao, H. Park, S.C. Chou, S.S. Karuppagounder, G.E. Umanah, S.P. Yun, et al., Poly (ADP-ribose) drives pathologic α -synuclein neurodegeneration in Parkinson's disease, *Science* 362 (6414) (2018) eaat8407, <https://doi.org/10.1126/science.aat8407>.
- [38] R.H. Kamel, A.A. AL-Tae, Iron oxide nanoparticles induced histological alteration and fetal skeletal abnormalities in the embryo of albino rats, *Med. -Leg. Update* 20 (1) (2020) 911–915, <https://doi.org/10.37506/mlu.v20i1.486>. Available at: (<http://ijop.net/index.php/mlu/article/view/486>).
- [39] A.Y. Lee, B.R. Hwang, M.H. Lee, S. Lee, E.J. Cho, Perilla frutescens var. japonica and rosmarinic acid improve amyloid- β 25–35 induced impairment of cognition and memory function, *Nutr. Res. Pract.* 10 (2016) 274–281, <https://doi.org/10.4162/nrp.2016.10.3.274>.
- [40] F. Li Pomi, V. Papa, F. Borgia, M. Vaccaro, A. Allegra, N. Cicero, S. Gangemi, *Rosmarinus officinalis* and skin: antioxidant activity and possible therapeutic role in cutaneous diseases, *Antioxidants* 12 (3) (2023) 680, <https://doi.org/10.3390/antiox12030680>.
- [41] K.J. Livak, T.D. Schmittgen, Analysis of relative gene expression data using real-time quantitative PCR and the 2(-Delta Delta C(T)) Method, *Methods* 25 (4) (2001) 402–408, <https://doi.org/10.1006/meth.2001.1262>.
- [42] N. Malhotra, J.-S. Lee, R.A.D. Liman, J.M.S. Ruallo, O.V. Villaflores, T.-R. Ger, C.-D. Hsiao, Potential toxicity of iron oxide magnetic nanoparticles: a review, *Molecules* 25 (14) (2020) 3159, <https://doi.org/10.3390/molecules25143159>.
- [43] N.V. Maluchenko, A.V. Feofanov, V.M. Studitsky, PARP-1-associated pathological processes: inhibition by natural polyphenols, *Int. J. Mol. Sci.* 22 (21) (2021) 11441, <https://doi.org/10.3390/ijms222111441>.
- [44] J.M. Marcus, M.L. Hossain, J.P. Gagné, G.G. Poirier, L.L. McMahon, R.M. Cowell, S. A. Andrabi, PARP-1 activation leads to cytosolic accumulation of TDP-43 in neurons, *Neurochem. Int.* 148 (2021) 105077, <https://doi.org/10.1016/j.neuint.2021.105077>.
- [45] E.K. Mohamed, M.M. Fathy, N.A. Sadek, et al., The effects of rutin coat on the biodistribution and toxicities of iron oxide nanoparticles in rats, *J. Nanopart. Res.* 26 (2024) 49, <https://doi.org/10.1007/s11051-024-05949-w>.
- [46] A. Mohammed FE, T.T. Mohammed, A.A. Mohamed, A.A. Shaaban, A. Atwa, The possible protective roles of garlic oil and rosemary extract against neuro and geno/toxicities of acrylamide on adult male albino rats, *Zagazig J. Forensic Med. Toxicol.* 18 (1) (2020) 68–90. (https://zjfm.journals.ekb.eg/article_67154_b8f849df15ee15bfe9af87a5aad8d668.pdf) (Avilable at).
- [47] A.R. Monteiro, D.J. Barbosa, F. Remião, R. Silva, Alzheimer's disease: Insights and new prospects in disease pathophysiology, biomarkers and disease-modifying drugs, *Biochem. Pharmacol.* 211 (2023) 115522, <https://doi.org/10.1016/j.bcp.2023.115522>.
- [48] M.G. Montiel Schneider, M.J. Martín, J. Otarola, E. Vakarelska, V. Simeonov, V. Lassalle, M. Nedyalkova, Biomedical applications of iron oxide nanoparticles: current insights progress and perspectives, *Pharmaceutics* 14 (1) (2022) 204, <https://doi.org/10.3390/pharmaceutics14010204>.
- [49] R.D. Moura, P.D. Mattos, P.F. Valente, N.C. Hoch, Molecular mechanisms of cell death by parthanatos: more questions than answers, *Genet. Mol. Biol.* 471 (1) (2024) e20230357, <https://doi.org/10.1590/1678-4685-GMB-2023-0357>.
- [50] E. Naderali, F. Nikbakht, S.N. Ofogh, H. Rasoolijazi, The role of rosemary extract in degeneration of hippocampal neurons induced by kainic acid in the rat: a behavioral and histochemical approach, *J. Integr. Neurosci.* 17 (1) (2018) 19–25, <https://doi.org/10.31083/JIN-170035>.
- [51] National Research Council, *Guide for the Care and Use of Laboratory Animals*, National Academies Press (US), Washington (DC), 1996, <https://doi.org/10.17226/5140>.
- [52] J. Nowak-Jary, B. Machnicka, Comprehensive analysis of the potential toxicity of magnetic iron oxide nanoparticles for medical applications: cellular mechanisms and systemic effects, *Int. J. Mol. Sci.* 25 (22) (2024) 12013, <https://doi.org/10.3390/ijms252212013>. PMID: 39596080; PMCID: PMC11594039.
- [53] A.M. Ojeda-Sana, C.M. van Baren, M.A. Elechosa, M.A. Juárez, S. Moreno, New insights into antibacterial and antioxidant activities of rosemary essential oils and their main components, *Food Control* 31 (2013) 189–195, <https://doi.org/10.1016/j.foodcont.2012.09.022>.
- [54] S. Pazzaglia, C. Pioli, Multifaceted Role of PARP-1 in DNA repair and inflammation: pathological and therapeutic implications in cancer and non-cancer diseases, *Cells* 9 (1) (2019) 41, <https://doi.org/10.3390/cells9010041>.
- [55] J.R. Prohaska, A.A. Gybina, Rat brain iron concentration is lower following perinatal copper deficiency, *J. Neurochem.* 93 (3) (2005) 698–705, <https://doi.org/10.1111/j.1471-4159.2005.03091.x>.
- [56] R. Qiao, C. Fu, H. Forgham, I. Javed, X. Huang, J. Zhu, A.K. Whittaker, T.P. Davis, Magnetic iron oxide nanoparticles for brain imaging and drug delivery, *Adv. Drug Deliv. Rev.* 197 (2023) 114822, <https://doi.org/10.1016/j.addr.2023.114822>.
- [57] M.G. Rahbardar, H. Hosseinzadeh, Therapeutic effects of rosemary (*Rosmarinus officinalis* L.) and its active constituents on nervous system disorders, *Iran. J. Basic Med. Sci.* 23 (9) (2020) 1100–1112, <https://doi.org/10.22038/ijbms.2020.45269.10541>.
- [58] U.A. Reddy, P.V. Prabhakar, M. Mahboob, Biomarkers of oxidative stress for in vivo assessment of toxicological effects of iron oxide nanoparticles, *Saudi J. Biol. Sci.* 24 (6) (2017) 1172–1180, <https://doi.org/10.1016/j.sjbs.2015.09.029>.
- [59] W. Ren, G. Jing, Q. Shen, X. Yao, Y. Jing, F. Lin, W. Pan, Occludin and connexin 43 expression contribute to the pathogenesis of traumatic brain edema, *Neural Regen. Res.* 8 (29) (2013) 2703–2712, <https://doi.org/10.3969/j.issn.1673-5374.2013.29.002>.
- [60] L. Sadeghi, A. Marefat, Investigation of the iron oxide nanoparticle effects on amyloid precursor protein processing in hippocampal cells, *Basic Clin. Neurosci.* 14 (2) (2023) 203–212, <https://doi.org/10.32598/bcn.2021.2005.1>.
- [61] P. Seyedemadi, M. Rahnema, M.R. Bigdeli, S. Oryan, H. Rafati, The neuroprotective effect of rosemary (*Rosmarinus officinalis* L.) hydro-alcoholic extract on cerebral ischemic tolerance in experimental stroke, *Iran. J. Pharm. Res.* 15 (4) (2016) 875–883. PMID: 28243285.
- [62] A. Singh, R. Kukreti, L. Saso, S. Kukreti, Oxidative stress: a key modulator in neurodegenerative diseases, *Molecules* 24 (8) (2019) 1583, <https://doi.org/10.3390/molecules24081583>.
- [63] F. Tietze, Enzymic method for quantitative determination of nanogram amounts of total and oxidized glutathione: applications to mammalian blood and other tissues, *Anal. Biochem.* 27 (3) (1969) 502–522, [https://doi.org/10.1016/0003-2697\(69\)90064-5](https://doi.org/10.1016/0003-2697(69)90064-5).
- [64] R. Vakili-Ghartavol, A.A. Momtazi-Borojeni, Z. Vakili-Ghartavol, et al., Toxicity assessment of superparamagnetic iron oxide nanoparticles in different tissues, *Artif. Cells Nanomed. Biotechnol.* 48 (1) (2020) 443–451, <https://doi.org/10.1080/21691401.2019.1709855>.
- [65] G.S. Verma, N.K. Nirmal, D. Gunpal, H. Gupta, M. Yadav, N. Kumar, P.J. John, Intraepiteneal exposure of iron oxide nanoparticles causes dose-dependent toxicity in Wistar rats, *Toxicol. Ind. Health* 37 (12) (2021) 763–775, <https://doi.org/10.1177/07482337211058668>.
- [66] Wang H., Cheng J., Yang S., Cui S.W., Wang M., Hao W. (2020) Rosemary extract reverses oxidative stress through activation of Nrf2 signaling pathway in hamsters fed on high fat diet and HepG2 cells. *JFF.* 74:104136. doi: 10.1016/j.jff.2020.104136.
- [67] P.L. Wencel, W.J. Lukiw, J.B. Strosznajder, R.P. Strosznajder, Inhibition of poly (ADP-ribose) polymerase-1 enhances gene expression of selected sirtuins and APP cleaving enzymes in amyloid beta cytotoxicity, *Mol. Neurobiol.* 55 (6) (2018) 4612–4623, <https://doi.org/10.1007/s12035-017-0646-8>.
- [68] L. Wu, W. Wen, X. Wang, D. Huang, J. Cao, X. Qi, S. Shen, Ultrasmall iron oxide nanoparticles cause significant toxicity by specifically inducing acute oxidative stress to multiple organs, *Part. Fibre Toxicol.* 19 (1) (2022) 24, <https://doi.org/10.1186/s12989-022-00465-y>.
- [69] Y. Yao, J. Mao, S. Xu, L. Zhao, L. Long, L. Chen, D. Li, S. Lu, Rosmarinic acid inhibits nicotine-induced C-reactive protein generation by inhibiting NLRP3 inflammasome activation in smooth muscle cells, *J. Cell Physiol.* 234 (2019) 1758–1767, <https://doi.org/10.1002/jcp.27046>.

- [70] J.F. Ying, Z.B. Lu, L.Q. Fu, Y. Tong, Z. Wang, W.F. Li, X.Z. Mou, The role of iron homeostasis and iron-mediated ROS in cancer, *Am. J. Cancer Res.* 11 (5) (2021) 1895–1912. PMID: 34094660.
- [71] M.H. Yu, J.H. Choi, I.G. Chae, H.G. Im, S.A. Yang, K. More, I.S. See, J. Lee, Suppression of LPS-induced inflammatory activities by *Rosmarinus officinalis* L, *Food Chem.* 136 (2013) 1047–1054, <https://doi.org/10.1016/j.foodchem.2012.08.085>.
- [72] Y. Zhao, L. Gan, L. Ren, Y. Lin, C. Ma, X. Lin, Factors influencing the blood-brain barrier permeability, *Brain Res.* 1788 (2022) 147937, <https://doi.org/10.1016/j.brainres.2022.147937>.